On the Improvement of Electric Field Energy Harvesting from Domestic Power Lines

Jiafeng Zhou[a,*], Jinyao Zhang[a], Chen Xu[a], Le Fang[a], Ye Wang[a], Yuan Zhuang[a], Tianyuan Jia[a], Huang Yi[a], Congzheng Han[b,*]

[a] *Department of Electrical Engineering and Electronics, University of Liverpool, Liverpool, L69 3GJ, U.K.*
[b] *Institute of Atmospheric Physics, Chinese Academy of Sciences, Beijing, China*

ARTICLE INFO

Keywords:
Electric field energy harvesting
Rectifier circuit
Switching circuit

ABSTRACT

A method to improve electric field energy harvesting (EFEH) from domestic power lines by 100% is proposed in this paper. Making use of the electric field around power lines is a promising way to harvest ambient energy. One common method is to use a copper sheet to wrap on the insulator of a power line. The capacitance between the copper sheet and the live wire is utilized to extract energy. However, this parasitic capacitance would limit the output power of such a harvester as well when a full bridge rectifier is used. To deal with this problem, a new method is proposed to improve the harvested energy by using a switching circuit. By monitoring the output of a sensing circuit, the switching circuit shortens the discharging time of the parasitic capacitor and increases the output power. Compared with a conventional harvester, the proposed system can double the output power in theory. Theoretical calculations and experimental validations are presented to prove the concept. Measurement results show that the proposed harvester of a 90 cm long copper sheet wrapped on a domestic 230 V power line can harvest 367.5 μW power with 95.6% improvement.

1. Introduction

With the development of the Smart Grid, wireless sensor networks have been widely used to monitor high voltage power lines and utility assets. A wireless sensor node powered by a battery cannot work for a long time. Replacements of the batteries for these wireless sensor nodes are difficult and costly. As a result, the ability of the nodes to be self-powered is in high demand for such systems. Energy harvesting technology provides an alternative solution to batteries, which can convert ambient energies in the environment into electrical energy [1][2].

Energy harvesting is a technique that allows scavenging of stray energy present in the environment. A study has shown that systems or devices requiring mean power levels of 200 μW to about 10 mW can be powered from ambient sources [3]. There are various methods and sources that can be used to harvest energy, such as thermal energy [4], wind energy [5], tidal energy [6], RF energy [7], piezoelectric energy [8], magnetic field [9], electric field [10], *etc*. However, solar energy and wind energy cannot provide reliable power under some extreme weather conditions when the monitor system is needed the most. Electromagnetic energy harvesting technology is a very promising solution as it can provide continuous and reliable power under such conditions.

Any energized conductor emits a radial electric field that contains energy. Electric field energy harvesting (EFEH) circuit can be designed to collect this energy via capacitive displacement current that flows from the conductor to the ground. Based on that principle, a tube with a diameter of 30 cm and a length of 55 cm was mounted on the conductor as the first EFEH in study [11].

In previous work, [12] focused on theoretical and simulation analysis. [13] proposed a new type of electric field energy harvester based on electret electrostatic enhancement effect to harvest electric field energy. [14] described a power source of the condition monitoring devices for high-voltage transmission lines based on EFEH, and its energy harvesting ability in different sizes and installation positions was studied. [15] reported on an EFEH circuit, where the displacement current charged a large capacitor through a full-bridge diode rectifier, and the obtained energy directly supplied an antenna pack. This prototype provided 17 mW of continuous power from a 35 kV power line in the lab. However, the parasitic capacitance between harvests plates resulted in an input impedance of high value, lowering the dc/ac rectification efficiency of a full bridge rectifier. How to match the huge input impedance and achieve high output power are big issues in EFEH systems. [16] studied another solution in which a 50 or 60 Hz transformer was used to obtain power from a power source. The EFEH circuit needed a complicated control system to operate the switches in its conversion circuit. Therefore, the volume and weight issue were undesirable. [17] utilized LC resonator to solve the ac/dc conversion problem and increase the harvester power. With the upconversion oscillation circuit in this work, the 50 Hz voltage signal across the harvester can be converted into the signal envelop signal with an envelope frequency of 200 Hz. Hence, the size of the transformer was significantly reduced. The circuit exhibited high efficiency, but only achieved low output power. Furthermore, [18] proposed an EFEH harvester based on an insulator, which used a self-triggered discontinuously operating flyback converter to replace the conventional full bridge rectifier to transform ac power to useful low-voltage levels. However, their design needed to add a copper cube into the insulator, which could cause safety hazards. [19] showed a capacitive EFEH harvester that used a MEMS switch to manage the harvested energy. However, the "sleep mode" took at least 300 s, which was only suitable for sensors having limited working time, such as temperature sensors.

In this paper, an EFEH with a switching circuit is proposed. By turning on/off the switch periodically, the proposed system can overcome the limitation of parasitic capacitance to a conventional full-bridge rectifier. Based on this, the output power can be nearly doubled. The EFEH was implemented on a domestic power line to prove the concept.

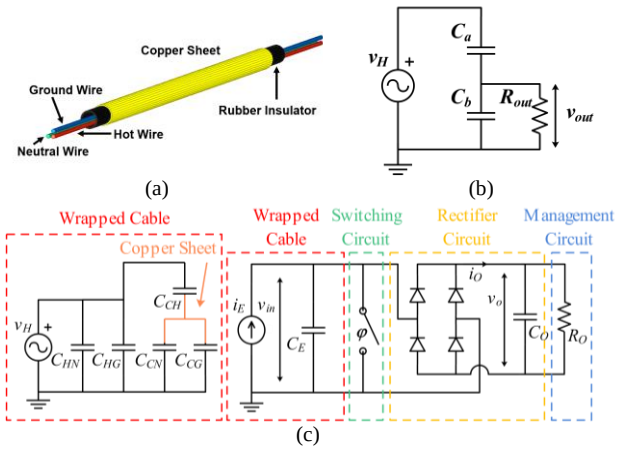

Fig.1. (a) Diagram of the EFEH on a domestic power line. (b) Equivalent circuit of the EFEH. (c) Schematic diagram of the proposed EFEH circuit.

The rest of this paper is organized as follows. Section II presents the E-field energy harvesting basics, followed by Section III, where the proposed EFEH system with a switching circuit is presented. In Section IV, a management circuit is proposed to match the output impedance. Section V presents the development of the proposed EFEH system, along with experimental results on a 230 V household power line. Section VII concludes this paper.

2. The Proposed EFEH Circuit

As shown in Fig. 1, the proposed EFEH system consists of three parts: a copper sheet wrapped on a power line, a switching circuit and a rectifier circuit. An insulated domestic power line is wrapped up by a copper sheet to construct parasitic capacitors. The capacitances between the surrounding copper sheet and the hot wire, neutral wire and safety ground wire in the line are denoted as C_{CH}, C_{CN} and C_{CG}, respectively. Due to the existence of C_{CH}, the voltage variation on the live wire will induce an ac voltage on the copper sheet. The equivalent circuit is shown in Fig. 1(b), where $C_a = C_{CH}$ and $C_b = C_{CN} + C_{CG} = 2C_a$. The copper sheet can then be regarded as a voltage source. The displacement current produced by the wrapped line can be utilized for energy harvesting [19].

The equivalent circuit of the wrapped power line is shown on the left side of Fig. 1(c). Since the geometry of the domestic power line is almost symmetric to the centre, the capacitance values of C_{CH}, C_{CN} and C_{CG} can be regarded as the same: $C_{CH} = C_{CN} = C_{CG}$. Both C_{HN} and C_{HG} are in parallel with the voltage source. The voltage source can be regarded as the same with or without these two capacitors. So they are omitted in the subsequent analysis. The nominal voltage between the live wire and the other two wires is 230 V_{rms} in the UK (50 Hz). The voltage source of the EFEH system can be converted to a capacitive current source as shown on the right side of Fig. 1(c), where the equivalent current source, input capacitor and input voltage are denoted as i_E, C_E and v_{in}, respectively. i_E is equal to $j\omega C_E v_{in}$, where ω is the angular frequency of the ac voltage. v_{oc} is the open-circuit voltage on C_b of the equivalent circuit when there is no load added in the EFEH system as shown in Fig. 1(b). Therefore, $v_{oc} = v_H/3$ and $C_E = C_a + C_b = 3C_a$.

The displacement current generated by the copper sheet can be used to harvest energy when a resistive load is connected between the copper sheet and the ground as shown in Fig. 1(b). According to [20], the ac output voltage V_{out} on the load resistor R_{out} can be expressed as:

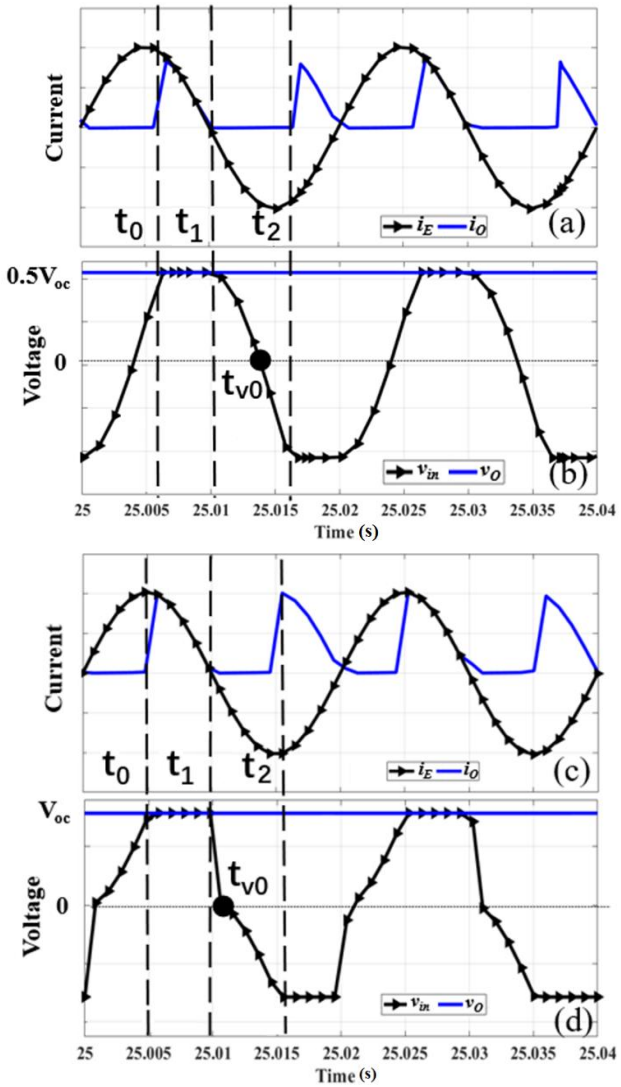

Fig.2. Waveforms of (a) i_E and i_o, (b) v_{in} and v_o on the conventional EFEH circuit; waveforms of (c) i_E and i_o, (d) v_{in} and v_o on the proposed EFEH circuit with respect to operating time.

$$V_{out} = \frac{\dfrac{\dfrac{R_{out}}{j\omega C_b}}{\dfrac{1}{j\omega C_b}+R_{out}}}{\dfrac{1}{j\omega C_a}+\dfrac{\dfrac{R_{out}}{j\omega C_b}}{\dfrac{1}{j\omega C_b}+R_{out}}} V_H = \frac{\omega C_a R_{out} V_H}{\omega R_{out}(C_a+C_b)-j} \quad (1)$$

where ω is the angular frequency of the ac voltage and V_H, V_{in} and V_{out} are the magnitude values of v_H, v_{in} and v_{out}, respectively. The absolute value of V_{out} can be calculated from (1), and can be expressed as:

$$|V_{out}| = \frac{\omega C_a R_{out} V_H}{\sqrt{1+\omega^2 {R_{out}}^2 (C_a+C_b)^2}} \quad (2)$$

Hence, the real power on the load can be expressed as:

$$P = \frac{|V_{out}|^2}{R_{out}} = \frac{\omega^2 {C_a}^2 R_{out} {V_H}^2}{1+\omega^2 {R_{out}}^2 (C_a+C_b)^2} \quad (3)$$

When $\partial P/\partial R_{out} = 0$, the ac output power of the conventional harvester will reach its peak, which can be expressed as:

$$\frac{\partial p}{\partial R_{out}} = \frac{\omega^2 {C_a}^2 {V_H}^2}{\omega^2 {R_{out}}^2 (C_a+C_b)^2+1} - \frac{2\omega^4 {C_a}^2 {V_H}^2 {R_{out}}^2}{\left(\omega^2 {R_{out}}^2 (C_a+C_b)^2+1\right)^2} = 0 \quad (4)$$

Substituting (4) into (3), the peak value can be expressed as:

$$P_{ac\_con} = \frac{\omega {C_a}^2 {V_H}^2}{2(C_a+C_b)} \quad (5)$$

and the optimal load resistance can be expressed as

$$R_{out} = \frac{1}{\omega(C_a+C_b)} = \frac{1}{\omega C_E} \quad (6)$$

However, due to the existence of C_E, if a rectifier is added to the EFEH system, the dc output power will be much lower than the maximum ac output power level given by (5). The displacement current generated on the copper sheet will flow through the full-bridge rectifier into the output capacitor C_o, as shown on the right side of Fig. 1(c). When the harvester circuit as shown in Fig. 1(c) is in the open circuit scenario (not connected to the management circuit), v_{in} will be equal to v_H /3. Meanwhile, v_o will be charged to V_{oc}, the peak value of v_{in}, which is equal to $\sqrt{2}V_H/3$. Without the proposed switching circuit, the steady-state waveforms on the EFEH circuit are shown in Fig. 2. When v_{in} increases from 0 V, the voltage on the output capacitor C_o is denoted as v_o. When v_{in} is lower than v_o, i_E flows into C_E to charge it. In this interval, all diodes in the full-bridge rectifier are reverse-biased and no current flows into the output capacitor C_o, until the voltage across the internal capacitor C_E reaches v_o. When this happens, two diodes in the full-bridge rectifier turns on and the current starts flowing into the output capacitor and the load. This condition continues until the current i_E changes direction.

Then the harvested energy will discharge C_E and then charge it to the opposite polarity. The whole sequence is repeated periodically. The total amount of charge available from the EFEH every cycle can be expressed as [21][22]

$$Q_{available/cycle} \int_0^{2\pi/\omega} |i_E|\, dt = \frac{4I_E}{\omega} = 4C_E V_{oc} \quad (7)$$

where ω is the angular frequency of the displacement current, and the equivalent current source can be represented as

$$i_E = I_E sin\omega t \quad (8)$$

In these sequences, the harvested ac energy cannot be transferred to the dc output when v_{in} changes from its positive peak to the negative peak, which requires 7 ms (from t_1 to t_2 as shown in Fig. 2 (b)). From t_1 to t_{v0}, v_{in} decreases from its positive peak to zero while C_E is being discharged. In this interval, the charges from the current source are wasted, which limits the output power of the EFEH circuit. The amount of the lost charges in a current cycle can be expressed as

$$Q_{lost\_conv} = 2C_E\big(V_o - (-V_o)\big) = 4C_E V_o \quad (9)$$

As can be seen in the voltage waveform shown in Fig. 2(b), the charges can be delivered to the load when the voltage is in the flat region, such as the interval from t_0 to t_1. The charges that flow into the load per cycle can be expressed as:

$$\begin{aligned} Q_{load} &= Q_{available} - Q_{lost\_conv} \\ &= 4C_E(V_{oc} - V_o) \end{aligned} \quad (10)$$

As a result, the energy and average power delivered to the load can be derived as:

$$E = Q_{load} V_o \quad (11)$$

$$P_{conv} = fE = 4C_E f V_o (V_{oc} - V_o) \quad (12)$$

When dP/dV_o is equal to 0, the dc output power will reach its maximum. The optimal V_o can be obtained as:

$$V_{o\_opt} = \frac{1}{2} V_{oc} \quad (13)$$

Meanwhile

$$P_{conv} = \frac{{V_o}^2}{R_o} \quad (14)$$

Substituting (13) and (14) into (12), the maximum dc output power for the conventional EFEH circuit with a full bridge rectifier can be expressed as:

$$P_{conv\_max} = C_E f {V_{oc}}^2 \quad (15)$$

at

$$R_o = \frac{1}{4C_E f} \quad (16)$$

According to (5) and (15), the ratio of P_{conv_max} to P_{ac_con} can be

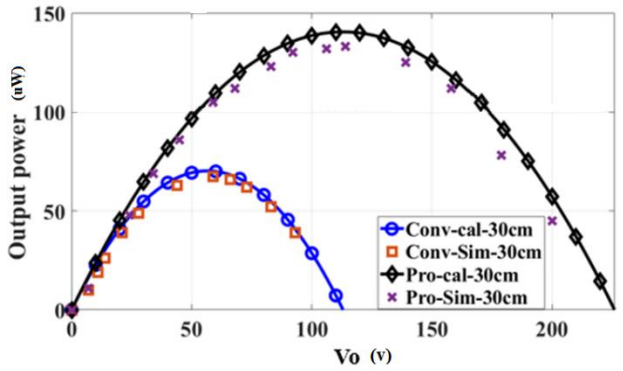

Fig. 3. The calculated and simulated output power of the conventional and the proposed methods, with respect to V_o. The copper sheet has a length of 30 cm. The value of V_o is controlled by changing the load resistance.

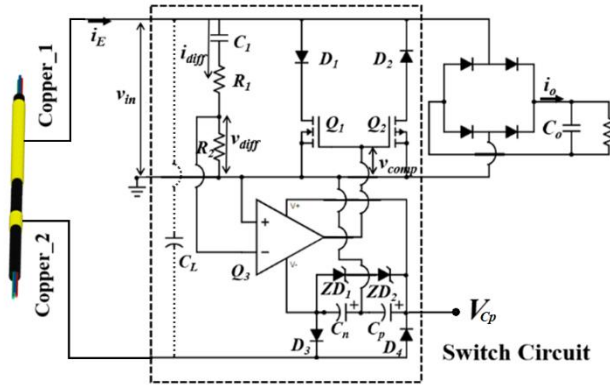

Fig. 4. Circuit diagram of the proposed switching circuit. It consists of a sensing circuit (C_1-R_1-R_2), a comparator (Q_3) and two branches of MOSFETs (D_1-Q_1 and D_2-Q_2). The output voltage of the sensing circuit, v_{diff}, is used to trigger Q_3. The output voltage of Q_3, v_{comp}, is used to control the switches Q_1 and Q_2.

expressed as:

$$\frac{P_{conv\_max}}{p_{ac\_con}} = \frac{C_E f {V_{oc}}^2}{\frac{\omega {C_a}^2 {V_H}^2}{2(C_a + C_b)}} \tag{17}$$

where $V_{oc} = \sqrt{2}V_H/3$, and$C_E = C_a + C_b = 3C_a$. According to (5) and (17), P_{conv_max} is calculated to be $2P_{ac\_con}/\pi$ in theory.

The available energy carried in the displacement current is wasted for 3.5 ms per half period (10 ms). In order to shorten the discharging time and increase the output power, a switching circuit is added in the EHEF system as shown in Fig. 1(c). The waveforms with the switching circuit are shown in Fig. 2(c) and (d). When v_{in} starts decreasing from its positive peak (or increasing from its negative peak), the switch turns on. Then C_E is short-circuited and v_{in} reaches zero instantaneously at $t_{vo} \approx t_1$. As a result, the discharging time can be shortened to zero in theory, and the output power would increase. According to Fig. 2(b), i_o is effective for a much longer time and v_o will charge to a higher peak value (about two times) than the results shown in Fig. 2(a).

The amount of the lost charges per cycle can be reduced to

$$Q_{lost\_pro} = C_E\big(V_o - (-V_o)\big) = 2C_E V_o \tag{18}$$

Similarly, the dc output power for the EFEH with the proposed switching circuit can be expressed as:

$$P_{pro} = 2C_E V_o f(2V_{oc} - V_o) \tag{19}$$

The maximum output power can be obtained as

$$P_{pro\_max} = 2C_E f {V_{oc}}^2 \tag{20}$$

at $V_o = V_{oc}$, and $R_o = 1/(2C_E f)$.

As a result, the peak of v_o (V_{o_peak}) will increase to twice the conventional EFEH circuit without the switching circuit. According to (5) and (20), P_{pro_max} can be $4P_{ac\_con}/\pi$ in theory. Thus the harvested power will be doubled compared to that of the conventional circuit.

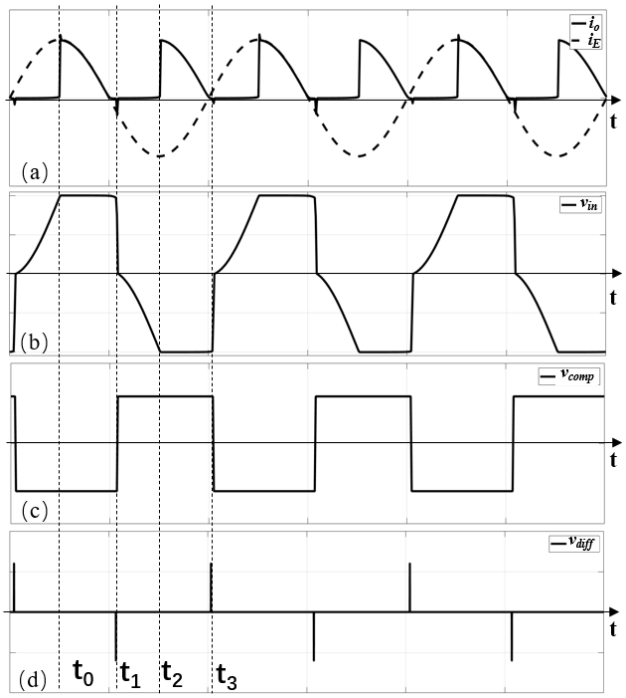

Fig. 5. Waveforms of (a) the source current i_E and output current i_o, (b) The input voltage v_{in}, (c) The output voltage of Q_3, and (d) The output voltage of the sensing circuit V_{diff} with respect to time.

In this study, the simulation packages Maxwell and Mutisim are used to evaluate the equivalent capacitance and simulate the proposed switching circuits, respectively. Fig. 3 shows the calculated and simulated results of the EFEH system using a wrapping copper sheet with a length of 30 cm. The equivalent capacitance C_E increases with the length of the wrapped copper. The output power is also a function of the load impedance. The maximum output power is achieved when v_o reaches its optimal value with the optimal load resistance. Then, the output power drops from its peak when the load impedance deviated from its optimal value. The conventional EFEH systems achieve their maximum dc output power when $V_{o\_peak} = 0.5V_{oc}$. An EFEH system with the proposed switching circuit can achieve its maximum output when $V_{o\_peak} = V_{oc}$, which is twice the conventional one. Since the optimal value of the load resistance is doubled as well, the dc output power is twice that of the conventional EFEH. The simulated results are in good agreement with the calculated ones. Therefore, the performance of the EFEH circuit is improved significantly by using the proposed switching circuit.

3. The Proposed Switching Circuit

To increase the output power extracted from a house-hold power line, a switch can be added as shown in the schematic diagram of Fig. 1(c). A control circuit is needed to operate the switch. The implemented switching control circuit is shown in Fig. 4. The switching circuit consists of a voltage sensing circuit (C_1-R_1-R_2), a comparator (Q_3) and two branches MOSFETs (D_1-Q_1 and D_2-Q_2). The switching circuit is connected to a copper sheet wrapped on the power line, copper_1.

As shown in Fig. 5, during the interval t_0 to t_1, v_{in} reaches the maximum value and is flat. The voltage on C_1 will be charged to the voltage of $0.5V_{oc}$ (or V_{oc} when the switching circuit is added) through R_1 and R_2. The voltage at the point between R_1 and R_2, v_{diff}, will be zero. When v_{in} decreases from the positive peak, v_{diff} becomes negative. Or v_{diff} will be positive when v_{in} increases from its trough.

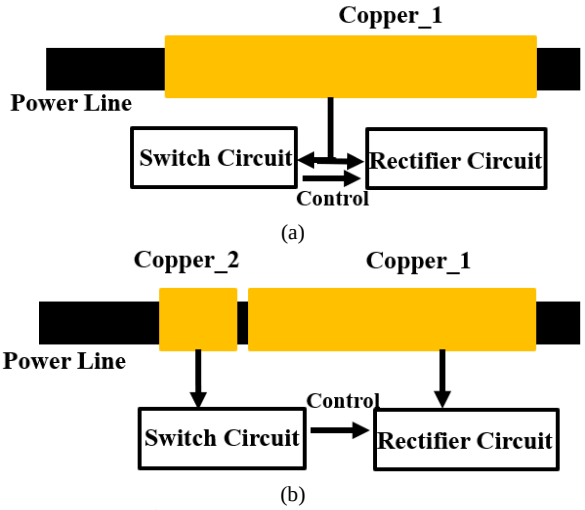

Fig. 6. Diagram of the proposed (a) one-section and (b) two-section EFEH.

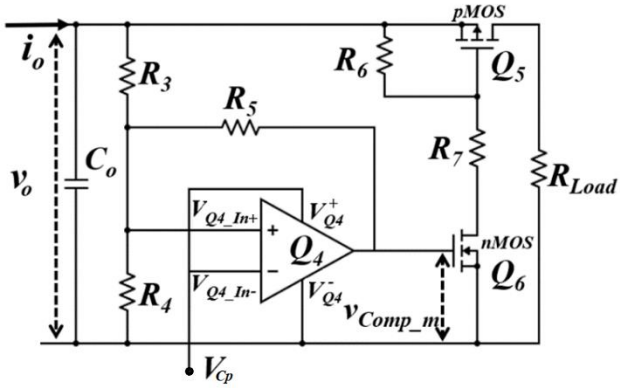

Fig. 7. The proposed power management circuit. It consists of a comparator (Q_4), two switches (Q_5 and Q_6), and five resistors (R_3, R_4, R_5, R_6 *and* R_7).

The values of R_1 and R_2 are chosen so that a suitable value of v_{diff} can be used as the input signal to trigger Q_3.

As shown in Fig. 5, during t_0 to t_1, the source current flows to the load via the full bridge rectifier. At time t_1, the source current i_E changes direction and v_{in} starts to drop from its maximum value. The sensing circuit generates a negative pulse at v_{diff}, which leads to a positive output of the comparator Q_3. Then, Q_1 turns on and the switching circuit is short-circuited to ground via D_1-Q_1. Q_2 is off at this interval. As a result, v_{in} drops from its peak value to zero at this instance. In the interval from t_1 to t_2, v_{in} decreases from 0 to the trough, Q_1 remains on and Q_2 remains off. There is no current on D_1-Q_1 since D_1 is reverse biased. There is no current on D_2-Q_2 as well since Q_2 is off. The output voltage of the comparator Q_3 (v_{comp}) keeps positive until i_E changes direction and v_{in} increases from the trough value. Then the sensing circuit will generate a positive pulse at time instance t_3. Q_2 turns on and the switching circuit is short circuited via D_2-Q_2. As a result, v_{in} drops from its peak value to zero at this instance. The whole sequence repeats periodically.

To power the comparator Q_3, a second copper sheet, copper_2, is wrapped on the power line, as shown in Fig. 4. Since the power consumption of the comparator is very low, a simple ac/dc rectification circuit was used. The ac voltage on the second cooper sheet is rectified by D_3 and D_4 to charge two storage capacitors C_n and C_p, respectively. Two Zener diodes ZD_1 and ZD_2 are connected in parallel with the two storage capacitors to limit the voltage and protect the circuit.

To realise the harvester, in fact, only one copper sheet is needed. As shown in Fig. 6(a), with the one-section method, copper_1 can also power the comparator Q_3 in the switching circuit. This can be achieved by charging the two storage capacitors C_n and C_p via a limiting capacitor (C_L) as shown in Fig. 4. However, in this case, v_{in} will be affected by the switching circuit, especially by the Zener diodes. One solution is to use a power manager circuit, so that only adequate power is distributed to power the comparator. Alternatively, with the two-section method as shown in Fig. 6(b), copper_2 is installed separately on the power line to charge the storage capacitors C_n and C_p. Since the power consumption of the nano-power comparator is very low compared with the harvested power, the length of copper_2 can be very short. The comparison of these two methods will be analyzed in Section 5.

4. The Management Circuit

To ensure sufficient energy can be accumulated to drive the load for practical applications and to reduce the magnitude of the optimal impedance of the load, a management circuit can be connected in parallel with C_o. According to (20), the optimal load impedance of the EFEH system is in the range of tens of MΩ. The proposed management circuit for the EFEH system is shown in Fig. 7. Resistors R_3, R_4 and R_5 are used to divide the voltage drop on C_o. Comparator Q_4 is used to switch the pMOS (Q_5) and the nMOS (Q_6). Resistors R_6 and R_7 are added to protect Q_5 and Q_6. Terminals V_{Q4_in-} and V^+_{Q4} are connected to V_{Cp}, one side of the storage capacitor C_p as shown in Fig. 4. V_{Cp} acts as both a reference input voltage and a power supply to provide dc power for the comparator.

When the harvester starts to work and C_o starts charging, the voltage v_o on C_o increases from 0 V. During the charging process, the output of the comparator (v_{comp_m}) is low and equal to V^-_{Q4}. The MOSFET switches Q_5 and Q_6 are off. When v_o reaches the upper bound voltage (V_{upper}), V_{Q4_in+} is equal to V_{Q4_in-} (or V_{Cp}). v_{comp_m} changes to a high value of V^+_{Q4}, which turns on Q_5 and Q_6. Since the value of v_{comp_m} becomes higher in this instant, the voltage of V_{Q4_in+} will be increased as well and much higher than V_{Cp}.

As a result, the energy stored in C_o will be discharged and delivered to the load. v_o gradually decreases from V_{upper} to the lower bound voltage (V_{lower}). When V_{Q4_in+} decreases to V_{Cp}, Q_5 and Q_6 will be turned off. C_o will no longer be discharged. Since the value of v_{comp_m} becomes lower in this instant, the voltage of V_{Q4_in+} will be decreased as well and much lower than V_{Cp}. Then the harvesting energy begins to accumulate in C_o again. The whole sequence repeats periodically.

The system generates an output pulse each cycle on the load. Therefore, the output impedance of the EFEH system can be reduced to a low value more suitable for practical applications, so that R_{load} can be chosen independently from the rectifier circuit.

5. Measured Results

To verify the proposed method, a copper sheet (copper_1) of 85 cm long is wrapped on an insulated power line to form an EFEH, as shown in Fig. 8. Another short cooper sheet copper_2 having a length of 5 cm is also wrapped on the power line to harvest power for the operation of the comparators in the switching circuit and the management circuit. The grounding of the circuit is provided by an oscilloscope, whose ground is connected to the earth. In the actual scenario, the grounding of the circuit can be the earth wire in the cable or the earth. The nominal voltage is 230 V at 50 Hz on a domestic power line in the UK. The power line has a diameter of 0.8 cm. The rubber insulator has a thickness of 0.18 cm. The live wire, ground wire and neutral wire have a diameter of 0.22 cm. For the conventional method, copper_1 has a length of 90 cm. The capacitance values of the parasitic capacitors C_{CN}, C_{CG} and C_{CH} are the same. The measured value of C_{CH} is 1.12 pF per cm so C_E is estimated to be 3.36 pF per cm. The estimated and simulated value of C_E is 302 pF and 307.8 pF, respectively, when copper_1 has a length of 90 cm.

The output capacitor C_o has a value of 1 μF. A low supply current comparator (Q_3: TLV3691), two MOSFET switches

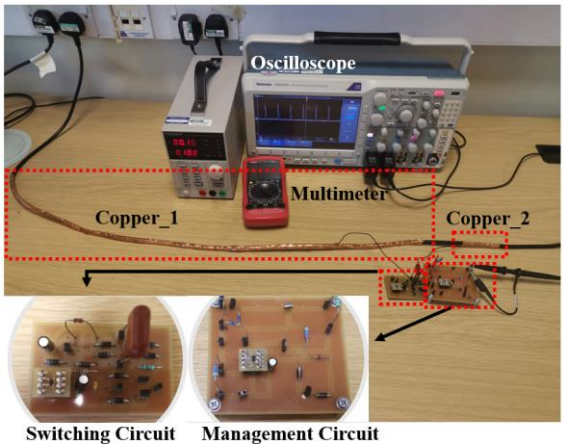

Fig. 8. The experimental setup. Copper_1 and Copper_2 have a length of 85 cm and 5 cm, respectively. The fabricated switching circuit and management circuit are also shown in the figure.

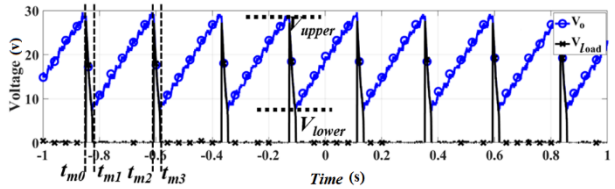

Fig. 9. The measured waveforms of v_{load} and the voltage on C_o.

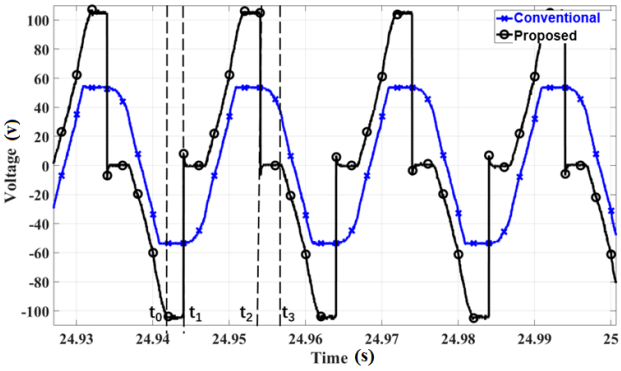

Fig. 10. Waveforms of v_{in} at C_E. The EFEH with the proposed one-section method and the conventional method were compared, when Copper_1 has a length of 90 cm.

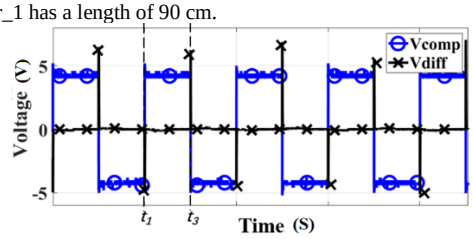

Fig. 11. Waveforms of the voltage at the output of the comparator Q_3 (V_{comp}) and the voltage at the output of the sensing circuit (V_{diff}).

(BSP372N and ZVP4424A) and two diodes (1N4007G) are used in the proposed switching circuit. A capacitor C_1 (2.2 pF) and two voltage dividing resistors (R_1 = 1 MΩ and R_2 = 1.5 MΩ) are added as the sensing circuit. Two storage capacitors C_n and C_p have a capacitance of 1 μF to provide dc power for comparator Q_3. Two Zener diodes (BZX79C4V7) are connected in parallel with the two storage capacitors to limit the voltage and protect the circuit.

A low supply current comparator (Q_4: TLV3701), two MOSFET switches (BSP126 and ZVP4424G) are used in the management circuit. Three voltage dividing resistors (R_3 = 200 MΩ, R_4 = 10.5 MΩ, R_5 = 12.5 MΩ) are added to set V_{upper} and V_{lower}. Two resistors (R_6 = 10 MΩ and R_7 = 50 MΩ) are added to protect the two MOSFET switches. A 135 kΩ resistor is added as the load of the EFEH system. The V_{upper} and V_{lower} were set to be 30 V and 5 V, respectively. The measured results of the voltage on C_o and V_{load} are

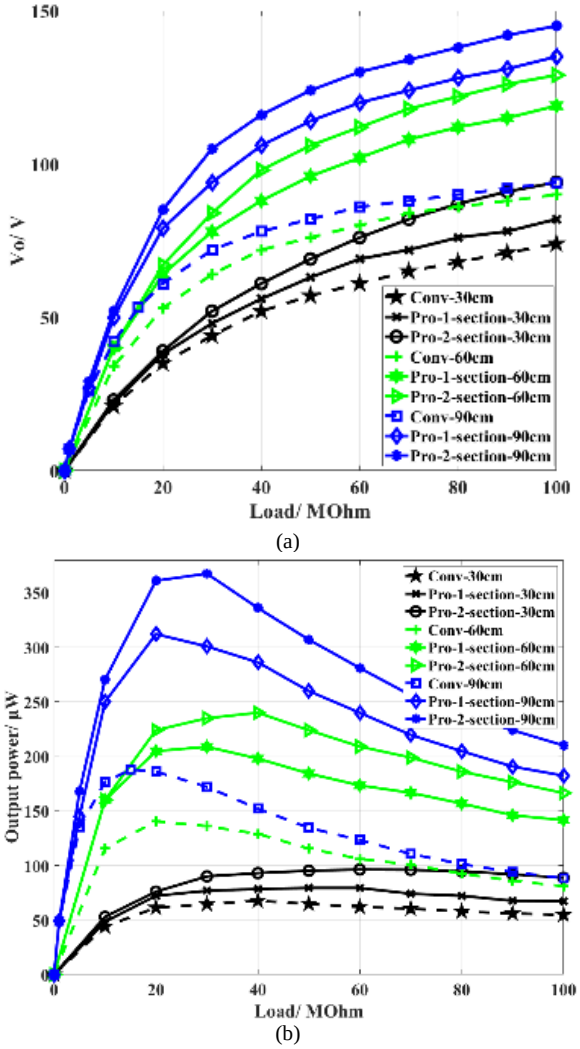

Fig. 12. The measured (a) V_o and (b) output power with respect to the load resistance. The measured results of the proposed one-section, two-section and conventional methods are compared with the calculated results, where the copper sheet has a total length of 30 cm, 60 cm and 90 cm, respectively.

shown in Fig. 9. It should be noted that V_{upper} and V_{lower} can be set to any desired values by choosing appropriate values for R_3, R_4 and R_5.

The measured v_{in} for the EFEH circuit is shown in Fig. 10. The output of the comparator is triggered by the output of the sensing circuit, to ensure that the switching circuit turns on when v_{in} changes from the positive peak or negative peak, as shown in Fig. 11. At time instance t_1, v_{diff} has a negative pulse, which leads to a positive output of the comparator Q_3. The switch is turned on, and v_{in} drops from its peak value to zero at this instance. As a result, the discharge time can be shortened, and the output power would increase. v_{comp} keeps positive until the sensing circuit generated a positive pulse at the time instance t_3.

According to Fig. 10, with the proposed switching circuit, v_{in} has a peak value of 105.1 V with an optimal load (30 MΩ). For the conventional method, V_{in} has a peak value of 53.1 V with an optimal load (15 MΩ). Compared with the conventional method, the maximum output power has been improved by 95.6% from 187.9 μW to 367.5 μW.

The measured voltage and output power with respect to the load resistance are shown in Fig. 12(a) and (b), respectively. As shown in Fig. 12(b), the maximum output powers achieved are 96.3 μW, 240 μW and 367.5 μW for the proposed two-section EFEH system with wrapped copper sheets having a total length of 30 cm, 60 cm and 90cm, respectively. Since copper_2 has a length of 5 cm, copper_1 is reduced by 5 cm accordingly in the proposed two-

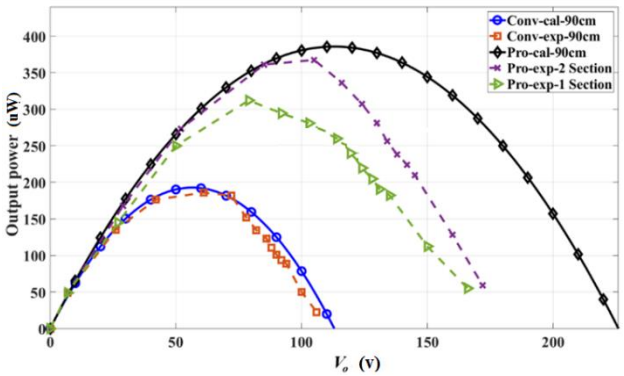

Fig.13. The measured output power with respect to V_o. The measured results of the proposed one-section, two-section and conventional methods (pro-exp-1 section, pro-exp-2 section and Conv-exp-90cm respectively) were compared with the calculated results (pro-cal-90cm and Conv-cal-90cm). The peak ac output power of the conventional method was denoted as P_{ac_con} (90cm).

Table 1
Comparison of Experimental results

	Output Power (μW)	V_o (V)	Improvement Compared with Conv-method
1-section-30 cm	79.4	69	17.4%
2-section-30 cm	96.3	76	42.5%
1-section-60 cm	208.8	79	48.6%
2-section-60 cm	240	98	70.1%
1-section-90 cm	312.1	79	66%
2-section-90 cm	367.5	105	95.6%

Table 2
Comparison with the-state-of-the-art

	Voltage on Power line	Equivalent Capacitor (C_E)	Maximum output power (Compared with the peak value of conventional ac output Power P_{ac_con})
[17]	10 kV	211.7 pF	663 μW (0.91 P_{ac_con})
[18]	12.7 kV	43 pF	23.6 mW (0.33 P_{ac_con})
	220 V	297 pF	194 μW (0.64 P_{ac_con})
This Work (1-section-90 cm)	**230 V**	**302.1 pF**	**312.1 μW (1.12 P_{ac_con})**
This Work (2-section-90 cm)	**230 V**	**286.4 pF**	**367.5 μW (1.32 P_{ac_con})**

section method.

The optimal load of the proposed two-section EFEH system is twice the load impedance of the conventional harvester. The measured output power with respect to v_o is shown in Fig. 13. The measured results are in good agreement with the calculated ones. **For the proposed two-section method, the EFEH system has a maximum output power of 367.5 μW when the voltage on the load is 100 V with a load impedance of 30 MΩ. The calculated maximum output power is 385.6 μW in the ideal case, so the rectification efficiency is 95.3%. The proposed method is slightly less efficient compared to the traditional method's result of 97% at 186 μW, but the output power is almost twice as high**.

With the one-section method, copper_1 and copper_2 are linked together as one piece. In this case, the maximum output power is 312.1 μW when the load impedance is 20 MΩ and the voltage on the load is 79 V. The output power is lower than the two-section case, although the total lengths of the copper are the same. This is because part of the energy on C_E is diverted into the storage capacitors C_n and C_p by a limiting capacitor C_L. As this part is not accurately managed, more than necessary power can be delivered to the switching and managing circuit. Also, the Zener diodes in the switching circuit would affect V_{in}, hence the output power. It is a simple and effective solution to use two sections as discussed above. Alternatively, another low power control circuit can be utilized to ensure no excessive power or voltage is provided to the switching and management circuit.

These results are in good agreement with the analytical results obtained in Section II. The measured results with different lengths of copper sheets are summarized in Table 1. The comparison with the state-of-the-art is shown in Table 2. [17] and [18] used an up-conversion oscillation circuit and flyback converter circuit to solve the ac/dc conversion problem in the EFEH system, respectively. However, the EFEH system in [17] requested three equivalent capacitors connected in series, which reduced the input voltage of their EFEH circuit. Although their circuit was installed on a 10 kV power line, the harvested power was quite low (663 μW), compared with 367.5 μW output power on 220 V power line in this work. The ac/dc conversion circuit in [18] was much more complicated than the proposed switch circuit in this paper. The maximum dc output powers achieved were $0.91p_{ac\_con}$ and $0.33p_{ac\_con}$ in [17] and [18], respectively, where p_{ac_con} is the maximum harvested ac power as calculated by (5). [19] showed an EFEH harvester using a MEMS switch on a 220 V / 60 Hz power line, whose power source was at a similar power level with the proposed work. However, this design only achieved $0.64p_{ac\_con}$ maximum output power. With the proposed switch circuit, the maximum harvested power was increased to $1.12p_{ac\_con}$ and $1.32p_{ac\_con}$ using the 1-section-method and 2-section-method, respectively.

6. Conclusion

To conclude, an EFEH system with a switching circuit has been proposed in this paper. The capacitance between a copper sheet wrapped on a power line and wires inside the power line can be utilised to harvest energy. But this capacitance limits the output power as well. By turning on/off the switch periodically, the proposed EFEH system can overcome the limitation. A sensing circuit is added to generate a signal to automatically control the switching circuit. The output power has been increased by 100% in theory. A management circuit is added to control the output voltage and lower the load impedance. The proposed fully self-contained harvester with a 90 cm long copper sheet wrapped on a domestic power line has harvested 367.5 μW output power with 95.6% improvement from the conventional system. The experimental results are in good agreement with the calculated ones.

References

[1] B. Ji, K. Song, C. Li, W.-p. Zhu, and L. Yang, "Energy harvest and information transmission design in internet-of-things wireless communication systems," *AEU - International Journal of Electronics and Communications*, vol. 87, pp. 124-127, Apr. 2018.

[2] O. P. Angwech, A. S. Alfa, and B. T. J. Maharaj, "Managing the harvested energy in wireless sensor networks: A priority Geo/Geo/1/k approach with threshold," Energy Reports, vol. 8, pp. 2448-2461, Nov. 2022.

[3] N. M. Roscoe and M. D. Judd, "Harvesting Energy From Magnetic Fields to Power Condition Monitoring Sensors," IEEE Sensors Journal, vol. 13, no. 6, pp. 2263-2270, Jun. 2013.

[4] R. I. S. Pereira, M. M. Camboim, A. W. R. Villarim, C. P. Souza, S. C. S. Jucá, and P. C. M. Carvalho, "On harvesting residual thermal energy from photovoltaic module back surface," *AEU - International Journal of Electronics and Communications*, vol. 111, p. 152878, Nov. 2019.

[5] X. Du, L. Du, X. Cai, Z. Hao, X. Xie, and F. Wu, "Dielectric elastomer wave energy harvester with self-bias voltage of an ancillary wind generator to power for intelligent buoys," *Energy Conversion and Management*, vol. 253, p. 115178, Feb. 2022.

[6] T. Zhao, M. Xu, X. Xiao, Y. Ma, Z. Li, and Z. L. Wang, "Recent progress in blue energy harvesting for powering distributed sensors in ocean," *Nano Energy*, vol. 88, p. 106199, Oct. 2021.

[7] X. N. Tran, V.-P. Hoang, and B. C. Nguyen, "Combining RF energy harvesting and cooperative communications for low-power wide-area systems," *AEU - International Journal of Electronics and Communications*, vol. 139, p. 153909, Sep. 2021.

[8] R. Srinivasan, U. Mangalanathan, and U. Gandhi, "Dual input buck-boost converter for hybrid piezoelectric energy harvester – Supercapacitor sources," *AEU - International Journal of Electronics and Communications*, vol. 111, p. 152926, Nov. 2019.

[9] S. Yuan, Y. Huang, J. Zhou, Q. Xu, C. Song and G. Yuan, "A High-Efficiency Helical Core for Magnetic Field Energy Harvesting," *IEEE Transactions on Power Electronics*, vol. 32, no. 7, pp. 5365-5376, Jul. 2017.

[10] O. Menéndez, S. Kouro, M. Pérez, and F. Auat Cheein, "Mechatronized maximum power point tracking for electric field energy harvesting sensor," *AEU - International Journal of Electronics and Communications*, vol. 110, p. 152830, Oct. 2019.

[11] H. Zangl, T. Bretterklieber and G. Brasseur, "A Feasibility Study on Autonomous Online Condition Monitoring of High-Voltage Overhead Power Lines," in *Proc. IEEE Transactions on Instrumentation and Measurement*, vol. 58, no. 5, pp. 1789-1796, May. 2009.

[12] F. Guo, H. Hayat and J. Wang, "Energy harvesting devices for high voltage transmission line monitoring," in *Proc. 2011 IEEE Power and Energy Society General Meeting*, Detroit, MI, USA, 2011, pp. 1-8.

[13] J. Zhang, J. Gu, X. Tian, D. Yan, D. Ou and J. Zhang, "Simulation of Electric Field Energy Harvesting Based on Electret Electrostatic Enhancement," in *Proc. 2021 4th International Conference on Energy, Electrical and Power Engineering (CEEPE)*, 2021, pp. 977-981.

[14] X. Zeng, Z. Yang, P. Wu, L. Cao and Y. Luo, "Power Source Based on Electric Field Energy Harvesting for Monitoring Devices of High-Voltage Transmission Line," *IEEE Transactions on Industrial Electronics*, vol. 68, no. 8, pp. 7083-7092, Aug. 2021.

[15] R. Moghe, A. R. Iyer, F. C. Lambert and D. Divan, "A Low-Cost Electric Field Energy Harvester for an MV/HV Asset-Monitoring Smart Sensor," *IEEE Transactions on Industry Applications*, vol. 51, no. 2, pp. 1828-1836, Mar.-Apr. 2015.

[16] M. Zhu, M. D. Judd, P. J. Moore and R. Zhang, "Energy harvesting technique for powering autonomous sensors within substations," in *Proc. 2009 International Conference on Sustainable Power Generation and Supply*, Nanjing, 2009, pp. 1-5.

[17] J. Zhang, P. Li, Y. Wen, F. Zhang and C. Yang, "A Management Circuit with Upconversion Oscillation Technology for Electric-Field Energy Harvesting," *IEEE Transactions on Power Electronics*, vol. 31, no. 8, pp. 5515-5523, Aug. 2016.

[18] J. C. Rodríguez, D. G. Holmes, B. Mcgrath and R. H. Wilkinson, "A Self-Triggered Pulsed-Mode Flyback Converter for Electric-Field Energy Harvesting," *IEEE Journal of Emerging and Selected Topics in Power Electronics*, vol. 6, no. 1, pp. 377-386.

[19] Kim, Hoseong, et al. "Stray electric field energy harvesting technology using MEMS switch from insulated AC power lines." *Electronics letters*, vol. 50, pp. 1236-1238, Aug. 2014.

[20] Zhao, Xinming, et al. "Energy harvesting for a wireless-monitoring system of overhead high-voltage power lines." *IET Generation, Transmission & Distribution*, vol. 7, no. 2, pp. 101-107, Feb. 2013.

[21] Y. Kumar. "Energy processing circuits for low-power applications." Diss. *Massachusetts Institute of Technology*, 2009.

[22] N. Krihely and S. Ben-Yaakov, "Self-Contained Resonant Rectifier for Piezoelectric Sources Under Variable Mechanical Excitation," *IEEE Transactions on Power Electronics*, vol. 26, no. 2, pp. 612-621, Feb. 2011.